



**HAL**  
open science

## **MACHe3, a prototype for non-baryonic dark matter search: KeV event detection and multicell correlation**

Clemens Winkelmann, E. Moulin, Yu. Bunkov, J. Genevey, Henri Godfrin, J.F.  
Macias-Perez, J.A. Pinston, D. Santos

### ► **To cite this version:**

Clemens Winkelmann, E. Moulin, Yu. Bunkov, J. Genevey, Henri Godfrin, et al.. MACHe3, a prototype for non-baryonic dark matter search: KeV event detection and multicell correlation. 39th Rencontres de Moriond - Cosmology : Exploring the Universe, Mar 2004, La Thuile, Italy. pp.71-76. <in2p3-00024105>

**HAL Id: in2p3-00024105**

**<https://in2p3.hal.science/in2p3-00024105v1>**

Submitted on 28 Apr 2005

**HAL** is a multi-disciplinary open access archive for the deposit and dissemination of scientific research documents, whether they are published or not. The documents may come from teaching and research institutions in France or abroad, or from public or private research centers.

L'archive ouverte pluridisciplinaire **HAL**, est destinée au dépôt et à la diffusion de documents scientifiques de niveau recherche, publiés ou non, émanant des établissements d'enseignement et de recherche français ou étrangers, des laboratoires publics ou privés.



HAL Authorization

**MACHE3,  
A PROTOTYPE FOR NON-BARYONIC DARK MATTER SEARCH:  
KeV EVENT DETECTION AND MULTICELL CORRELATION**

C. Winkelmann<sup>1</sup>, E. Moulin<sup>2</sup>,

Yu. Bunkov<sup>1</sup>, J. Genevey<sup>2</sup>, H. Godfrin<sup>1</sup>, J. Macías-Pérez<sup>2</sup>, J.A. Pinston<sup>2</sup>, D. Santos<sup>2</sup>

<sup>1</sup> *Centre de Recherches sur les Très Basses Températures, CNRS and Université Joseph Fourier,  
BP166, 38042 Grenoble cedex 9, France*

<sup>2</sup> *Laboratoire de Physique Subatomique et de Cosmologie, CNRS/IN2P3 and Université Joseph Fourier,  
53, avenue des Martyrs, 38026 Grenoble cedex, France*



MACHe3 (MAtrix of Cells of Helium 3) is a project for non-baryonic dark matter search using <sup>3</sup>He as a sensitive medium. Simulations made on a high granularity detector show a very good rejection to background signals. A multicell prototype including 3 bolometers has been developed to allow correlations between the cells for background event discrimination. One of the cells contains a low activity <sup>57</sup>Co source providing conversion electrons of 7.3 and 13.6 keV to confirm the detection of low energy events. First results on the multicell prototype are presented. A detection threshold of 1 keV has been achieved. The detection of low energy conversion electrons coming from the <sup>57</sup>Co source is highlighted as well as the cosmic muon spectrum measurement. The possibility to reject background events by using the correlation among the cells is demonstrated from the simultaneous detection of muons in different cells.

## 1 Introduction

From the latest results from observational cosmology experiments, the determination of the cosmological parameters has reached an unprecedented level of accuracy. Measurements of the cosmic microwave background (CMB) anisotropies <sup>1,2</sup> used in combination with large scale structures surveys and supernovae measurements point out that most of the matter is composed of non-baryonic dark matter. The leading candidates intended to explain this yet undiscovered component consist of new particles referred to as WIMPs (Weakly Interacting Massive Particles). Supersymmetric extensions of the standard model of particle physics provide a compelling dark matter candidate<sup>3</sup>, the lightest neutralino  $\tilde{\chi}$ , a neutral and colorless linear superposition of the superpartners of the gauge (B, W<sup>3</sup>) and Higgs (H<sub>d</sub><sup>0</sup>, H<sub>u</sub><sup>0</sup>) bosons.

Many collaborations have developed promising detectors to search for non-baryonic dark matter. These detectors have reached sufficient sensitivity to begin to test regions of the SUSY parameter space. Direct detection experiments present common problems such as the neutron interaction background and the radioactivity contamination from both the sensitive medium and the surrounding materials. Based on early experimental works, a superfluid  $^3\text{He}$  detector for direct detection of non-baryonic dark matter has been proposed<sup>4,5</sup>. First experimental tests of a  $^3\text{He}$  detector by neutrons and  $\gamma$ -rays have been done in Lancaster and Grenoble<sup>6,7,8</sup>. Monte Carlo simulations have demonstrated that a high granularity  $^3\text{He}$  detector would allow to reach high rejection factors against background events by using the measurement of the released energy together with the correlation among the cells<sup>9</sup>. Such a technique permits to obtain a low false neutralino event rate.

At ultra-low temperatures,  $^3\text{He}$  is a very appealing material because it constitutes a highly sensitive bolometer. At temperatures around  $100\ \mu\text{K}$ ,  $^3\text{He}$  is in its superfluid B phase for which the quasiparticle gap and the heat capacity are extremely small. The use of  $^3\text{He}$  profits of very interesting features with respect to other materials :

- $^3\text{He}$  being a  $1/2$  spin nucleus, a  $^3\text{He}$  detector will be mainly sensitive to the axial interaction, making this device complementary to existing ones, mainly sensitive to the scalar interaction. The axial interaction is largely dominant in all the SUSY region associated with a substantial elastic cross-section<sup>10</sup>.

- A close to absolute purity (nothing can dissolve in  $^3\text{He}$  at  $100\ \mu\text{K}$ ).

- A high neutron capture cross-section, leading to a large energy release through the nuclear reaction  $n + ^3\text{He} \rightarrow p + ^3\text{H} + 764\ \text{keV}$ . Neutron contamination has thus a clear signature<sup>9,7</sup>, well discriminated from a WIMP signal.

- Low Compton cross-section . No intrinsic X-rays.

- A high signal to noise ratio, due to the narrow energy range expected for a WIMP signal. The maximum recoil energy does only slightly depend on the WIMP mass, due to the fact that the target nucleus ( $m = 2.81\ \text{GeV}/c^2$ ) is much lighter than the incoming  $\tilde{\chi}$ . As a matter of fact, the recoil energy range needs<sup>9,10</sup> to be studied only below  $6\ \text{keV}$ .

## 2 Bolometric particle detection with superfluid $^3\text{He}$

### 2.1 Vibrating Wire Thermometry

A Vibrating Wire Resonator (VWR), sketched on the figure 1a, is a fine superconducting wire bent into semi-circular shape and oscillating perpendicularly to its plane. The oscillations are excited by a Laplace force in a uniform external magnetic field of about  $100\ \text{mT}$ , similarly to a loud-speaker. Typical resonant frequencies for the  $4.5\ \mu\text{m}$  diameter NbTi VWRs used are of about  $500\ \text{Hz}$ . The amplitude of the oscillations are detected via the voltage induced by the motion of the wire through the field lines. The signal is amplified by a cold transformer and a room-temperature low-noise pre-amplifier before being read out by a lock-in amplifier.

The dynamics of the VWR can be conveniently described by a damped harmonic oscillator model. The damping of the VWR is due to friction with the quasiparticles (QPs) of the surrounding superfluid<sup>11</sup>. Due to the presence of an isotropic superfluid gap of order  $\Delta = 0.14\ \mu\text{eV}$  in  $^3\text{He-B}$ , the QP density and thus the friction decrease exponentially as temperature is lowered. The resonance line-width at half-height  $W$  (figure 1b) is proportional to the QP-damping and related to temperature by  $W(T) = W_0 \exp(-\Delta/k_B T)$ . It exhibits an extremely steep temperature dependence around  $100\ \mu\text{K}$ . The measurement of  $W$  allows to access temperature with response times  $\tau_{\text{wire}} = 1/\pi W < 1\ \text{s}$ .

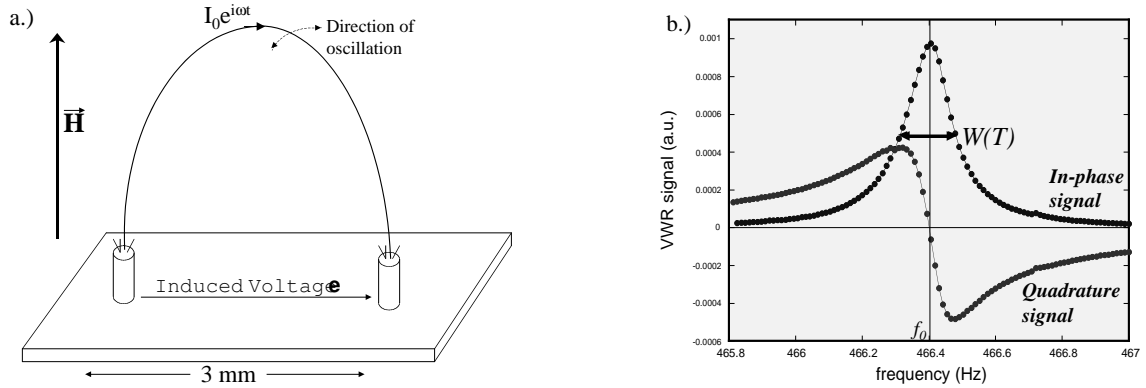


Figure 1: Setup for a monofilamentary NbTi Vibrating Wire (a). The induced signal is proportional to the oscillation amplitude and inversely proportional to the damping. The plot of a typical resonance sweep (b) with  $W(T)=170$  mHz indicates here a temperature of about  $120 \mu\text{K}$ .

## 2.2 $^3\text{He}$ bolometry

We use copper boxes of typical dimensions about 5 mm, filled with  $^3\text{He}$  which is in weak thermal contact with the outer bath through a small orifice. The interaction of a particle with the  $^3\text{He}$  in the box releases energy which results in an increase of the QP temperature, and thus density. The time constants for internal equilibrium of the quasi-particle gas are small ( $< 1$  ms). The time constant for thermal relaxation of QPs through the orifice after a heating event was tuned to be  $\tau_{box} \approx 5$  s. The heat leak through the container walls can be neglected because of the huge thermal resistance (Kapitza resistance) of solid-liquid interfaces at very low temperatures. Each box contains a least one VWR-thermometer which allows to follow rapid variations of the temperature.

In order to demonstrate the possibility of efficient background rejection by correlating many cells, we have built a 3-cell bolometer prototype, as sketched in the figure 2. One of the cells (C) contains an extra VWR, slightly larger, that allows to calibrate the bolometer by depositing a well controlled amount of heat during a short mechanical pulse. One of the key features of this setup is the presence of a low activity  $^{57}\text{Co}$  source in the cell B. By detecting the low energy electrons emitted by this source we show that we have achieved a detection threshold of the order of 1 keV.

## 3 Experimental results

### 3.1 Analysis method

The raw data (see figure 3) consists of a serie of peaks which corresponds to the energy released by particles interacting with the  $^3\text{He}$  inside the cell. A procedure has been developed to analyse the spectra. Important efforts have been done to perform a correct treatment of low energy events presenting a high rate of pile-up. The method is based on several steps. First, a wavelet denoising allows to reduce significantly the noise on the raw data. The baseline, corresponding to low frequency temperature fluctuations in the thermal bath, is then removed. An iterative fit including a peak flagging followed by a fit to a reference peak previously extracted from data, allows to retrieve the position, amplitude and signal to noise ratio (S/N) for each detected peak<sup>12</sup>.

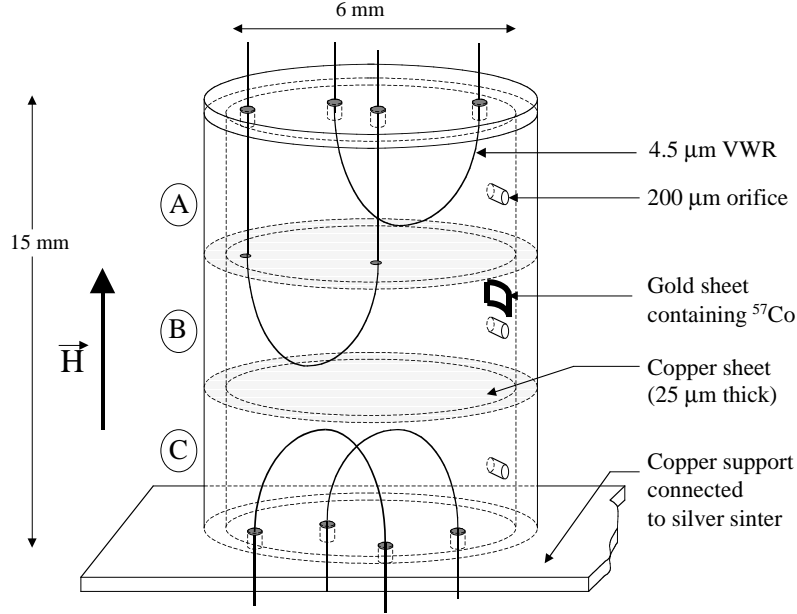


Figure 2: Experimental setup of the 3-cell bolometer. The 3 adjacent copper boxes are filled with superfluid  $^3\text{He}$  in weak thermal contact through the orifices with the outer bath, which acts as a thermal reservoir. Cell 'B' contains a low activity  $^{57}\text{Co}$  source (0.1 Bq). Cell 'C' contains an extra VWR for calibration.

### 3.2 Low energy spectrum from the low activity $^{57}\text{Co}$ source

In order to demonstrate the feasibility of detecting low energy events, a very low activity internal conversion electron  $^{57}\text{Co}$  source made in LPSC, deposited on a thin gold foil, has been embedded in one of the cells of the prototype as shown on figure 2. This low activity source ( $\sim 0.1$  Bq) provides electrons in the desired energy range ( $\sim 6$  keV). Data at  $100 \mu\text{K}$  have been taken during 18 hours. The dedicated analysis method allowed to obtain the low energy electron spectrum presented in figure 4. The low energy electron lines are clearly visible. The fact to see these confirms the very low background coming from the Compton interaction of the  $\gamma$ -rays (121 and 136 keV) of the source. The main spectrum structures have been identified from the nuclear desintegration scheme of the  $^{57}\text{Co}$  source. The main expected lines are reminded on figure 4. The spectrum is composed of two main components which correspond to the K shell and L shell internal conversion electrons of 14 keV nuclear transition respectively at 7.3 and 13.6 keV. Another contribution comes from the Auger electrons corresponding to the K and L shell. Different pile-ups are expected from the desintegration scheme. A line at 12.8 keV comes from the superposition of the K shell conversion electron with its corresponding 5.5 keV Auger electron. Two more peaks are observed at 21.7 and 27.9 keV. They result more likely from the 122 keV  $\gamma$ -ray interaction in the gold foil. Indeed, the L shell Auger electron from  $^{197}\text{Au}$  can pile-up with the K and L shell conversion electrons respectively. The background has been measured in the energy range of interest. It is shown on the right hand side plot on the figure 4. It is mainly composed of cosmic muons crossing the cell on peripheral tracks. Only two events on seven remain after multicell correlation between 1 and 6 keV. For further details, see E. Moulin *et al.*<sup>12</sup>.

### 3.3 Cosmic muons

Figure 5 (a) displays acquisition spectra from cells A and B. Events in coincidence are clearly visible. The correlation among the cells is proved to be a criteria for background rejection<sup>9</sup>. The



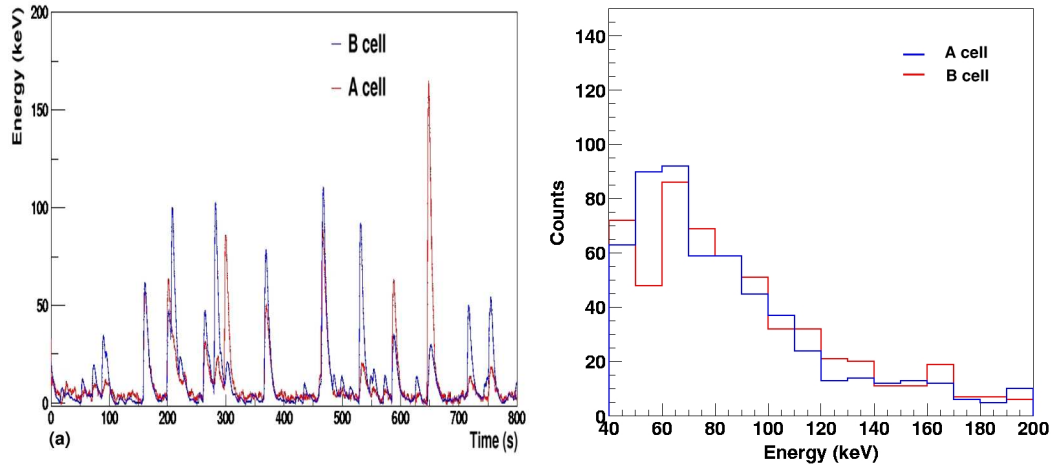


Figure 5: Acquisition data from cells A and B (a). Events in coincidence are clearly visible. They are composed of cosmic muons. The deposited energy by incident muons depends on the track length they make inside the cell. Cosmic muon detection in A and B cells (b). Spectra from cells A and B exhibit a peak at 65 keV.

peaks at 7.3 and 13.6 keV at 100  $\mu$ K is exhibited. Furthermore we demonstrate the possibility to improve background rejection by multicell correlation for a future detector.

## Acknowledgments

This project was partially funded by the Région Rhône-Alpes, by the European Community under the Competitive and Sustainable Growth programme (Contract G6RD-CT-1999-00119), by the Bureau National de Métrologie (Contract 00 3 004). Part of this work was done in the framework of the European Science Foundation scientific network "Coslab". E. Moulin wishes to acknowledge financial support from a European Union Grant for Young Scientists.

## References

1. D. Spergel *et al.*, *Astrophys. J. Sup.* **148**, 175 (2003)
2. A. Benoit *et al.*, *A&A* **Vol.399, No.3**, p.L25 (2003)
3. G. Jungman *et al.*, *Phys. Rept.* **267** 195 (1996)
4. G. Pickett, in Proc. "Second european workshop on neutrinos and dark matters detectors", ed by L. Gonzales-Mestres and D. Perret-Gallix, Editions Frontières, 1988, p. 377.
5. Yu. Bunkov, *et al.*, in Proc. "International Workshop Superconductivity and Particles Detection", ed by T. Girard, A. Morales and G. Waysand, World Scientific, 1995, p. 21.
6. D. Bradley *et al.*, *Phys. Rev. Lett.* **75**, 1887 (1995)
7. C. Bäuerle *et al.*, *Nature* (1995) **332**
8. C. Bäuerle *et al.*, *Phys. Rev. B* **57**, 22 (1998)
9. F. Mayet *et al.*, *Nucl. Instrum. Methods A* **455**, 554 (2000)  
E. Moulin *et al.*, to appear in Proc. of the 4th International Conference on "Where Cosmology and Fundamental Physics Meet", Marseille, June 2003, astro-ph/0309325
10. F. Mayet *et al.*, *Phys. Lett. B* **538**, 2002 (257)
11. S. Fisher *et al.*, *Phys. Rev. Lett.* **63**, 2566 (1989)
12. E. Moulin *et al.*, in preparation.
13. C. Winkelmann *et al.*, in preparation.